

1993

## Use of Near-Infrared Spectroscopy to Determine the Composition of High-Density/Low-Density Polyethylene Blend Films

Charles E. Miller  
*Haverford College*

Follow this and additional works at: [http://scholarship.haverford.edu/chemistry\\_facpubs](http://scholarship.haverford.edu/chemistry_facpubs)

---

### Repository Citation

Miller, Charles E. "Use of near-infrared spectroscopy to determine the composition of high-density/low-density polyethylene blend films." *Applied spectroscopy* 47.2 (1993): 222-228.

This Journal Article is brought to you for free and open access by the Chemistry at Haverford Scholarship. It has been accepted for inclusion in Faculty Publications by an authorized administrator of Haverford Scholarship. For more information, please contact [nmedeiro@haverford.edu](mailto:nmedeiro@haverford.edu).

# Use of Near-Infrared Spectroscopy to Determine the Composition of High-Density/Low-Density Polyethylene Blend Films

CHARLES E. MILLER\*

MATFORSK, Norwegian Food Research Institute, Osloveien 1, N-1430 Ås Norway

The ability of near-infrared (NIR) spectroscopy, combined with principal component regression (PCR), to nondestructively determine the blend ratio of high-density polyethylene (HDPE) and low-density polyethylene (LDPE) in extruded films is demonstrated. Results indicate that the NIR spectrum in the region 2100 to 2500 nm can be used to determine the HDPE mass percentage of 60–80- $\mu\text{m}$ -thick film samples to within 2.5%, over a range of 0 to 100%. NIR spectral effects from scattering are important for the determination of the HDPE % for HDPE contents above 50%, and spectral effects from changes in the methyl group concentration and perhaps the PE crystallinity are important for the determination of the HDPE % for HDPE contents below 50%. In addition, a large variation between the spectra of replicate samples, probably caused by variations in the degree or direction of molecular orientation in the samples, was observed.

Index Headings: Near-infrared; Polyethylene; Principal components regression.

## INTRODUCTION

Polyethylene (PE) is the major component of many food packaging products, including laminates, bags, and bottles. PE possesses the mechanical, optical, water-vapor-resistance, and heat-sealing properties that are very useful for food packaging applications.<sup>1–3</sup>

Although a PE molecule could be simply thought of as a long chain of connected ethylene units, real polyethylene polymers contain a significant number of side branches that are attached to the main polymer chains. Two commonly used types of PE, high-density polyethylene (HDPE) and low-density polyethylene (LDPE), refer to PE polymers that have relatively low and high degrees of branching, respectively. The amount of branching significantly affects the morphological properties of PE,<sup>4,5</sup> which in turn affects optical, physical, and thermal properties. Therefore, HDPE and LDPE have significantly different quality properties with respect to food packaging applications.

Recently, the strategy for preparation of polymeric materials for specific applications has focused on the blending of easily obtainable polymers. In the case of PE, studies have shown that the blending of HDPE and LDPE can result in materials that have morphological properties that are intermediate between those of pure HDPE and LDPE.<sup>4,6</sup> As a result, a special polyethylene with a specific quality can, in many cases, be prepared by simply blending two readily available PE materials.

For food packaging laminate applications, PE blends are commonly extruded into a thin film. Effective and

efficient quality assessment and process control for such films requires the frequent, and preferably nondestructive, determination of the relative amounts of HDPE and LDPE. FT-IR reflectance and transmission spectroscopy<sup>7</sup> can be used to perform such thin film analyses. However, because of the high absorptivities of IR bands, the film thickness must often be limited (up to approximately 50  $\mu\text{m}$ , depending on the specific IR bands used for the analysis) in order to perform an accurate quantitative analysis. Other IR methods, such as attenuated-total-reflectance (ATR)<sup>8</sup> and photoacoustic<sup>9,10</sup> methods, can provide IR spectra of optically thick materials, because they sample only a very thin layer at the surface of a material. However, it is important to note that the effective pathlength (or sampling depth) for the ATR and photoacoustic methods depends on the refractive index and thermal diffusivity of the material, respectively. Therefore, the use of these techniques for the quantitative analysis of nonhomogeneous materials, such as multi-layer laminate films, can be difficult.

If the optical thickness of a film sample is too large for FT-IR transmission analysis, then spectroscopy in the near-infrared (NIR) region can also be used for quantitative analysis.<sup>11,12</sup> Because NIR bands have lower absorptivities than IR bands, thicker and more highly scattering films can be sampled by NIR transmission than by IR transmission. In addition, the use of transmission spectroscopy for quantitative analysis can be accurately implemented through the Beer–Lambert law. Furthermore, NIR spectroscopy is easily adaptable to optical fibers,<sup>13,14</sup> which enable remote sampling for process or quality control analyses. Earlier works<sup>15–17</sup> have shown the usefulness of NIR spectroscopy for the nondestructive and noninvasive quality control of multi-layer laminate films.

The purpose of this work is to assess the ability of NIR spectroscopy to determine the percentage of HDPE in blend films of HDPE and LDPE.

## EXPERIMENTAL

**Materials.** Melt-extruded blend films of HDPE and LDPE at seven different blend ratios (0, 2.5, 5, 10, 25, 50, and 100% HDPE) were provided by STAT-OIL (Stathelle, Norway). For each of the seven different blend ratios, HDPE pellets (STAT-OIL H930,  $M_n = 35,000$ ,  $M_w = 223,000$ ,  $\text{CH}_2/1000\text{C} = 5$ ) and LDPE pellets (STAT-OIL L412,  $M_n = 29,900$ ,  $M_w = 215,000$ ,  $\text{CH}_2/1000\text{C} = 27$ ) were weighed and mechanically mixed before extrusion. Films were then prepared with a circular-die extruder (Windmüller and Hölcher, Varex 60.30D), with a 200-

Received 1 October 1992.

\* Present address: DuPont Polymers, Industrial Polymers Research, P.O. Box 1089, Building 10, Orange, TX 77631-1089.

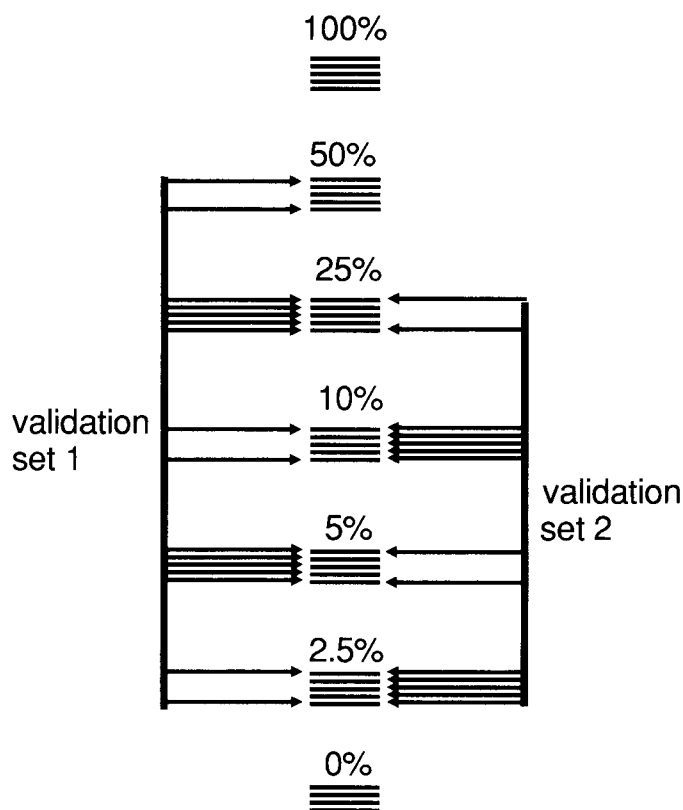


FIG. 1. Design of HDPE/LDPE blend film samples used for calibration, indicating the selection of the two cross-validation prediction sets. Percentages refer to HDPE %.

mm-diameter die and 1.2-mm die gap. The melt temperature and pressure depended on the blend ratio, and varied between 215 and 231°C and 174 and 278 bar, respectively. The blow-up ratio was 2.85 for all extrusions. After extrusion, the films were allowed to relax for 24 h before cutting. For each blend ratio, about 10 to 20 individual pieces were cut at various points along the extruded film. The resulting film pieces were approximately 30 cm × 30 cm and 25 to 40 μm thick. Observation of the films under polarized visible light indicated that they were highly oriented.

**Spectroscopy.** Five replicate NIR samples were prepared for each HDPE percentage. Because 25 to 40 μm is much less than the optimal sample thickness for NIR spectroscopy, each sample used in this analysis was in fact a “double-layer” of two 25- to 40-μm-thick pieces (where the two layers were obtained from two adjacently extruded pieces). Each sample was cut as a circle of approximately 3.5 cm diameter. They were then placed in an NIR reflective-transmission sample cell, with a gold-reflecting background and a glass cover. NIR reflective-transmission spectra were then collected over the region 2100 to 2500 nm in 2-nm increments, with the use of a Technicon InfraAnalyzer 500 NIR reflectance instrument (Technicon Instruments, Tarrytown, NY).

In order to study the effect of sample rotation on the NIR spectrum, a second series of samples were analyzed (five double-layer samples for each HDPE percentage). In this case, four replicate NIR scans of each sample were obtained in the following manner: after the first scan was obtained, the sample cell was rotated by ap-

proximately 45° (about the axis of the incident NIR light beam) and another scan was obtained; and two additional scans of the sample, rotated approximately 90° and 135° from its original position, were then obtained.

**Data Analysis.** Multiplicative scatter-correction (MSC)<sup>18</sup> was applied to the NIR spectra before multivariate modeling. The MSC-corrected spectra of the samples, and the known percentages of HDPE used in the different extrusions, were used to construct a principal component regression (PCR) (Unscrambler, CAMO A/S, Trondheim, Norway) calibration model that subsequently enables the prediction of the HDPE percentage of a PE film sample from its NIR spectrum. The calibration error (RMSEE) was determined as the root-mean-square of the differences between the known HDPE % values and the HDPE % values that were estimated from the PCR model.

Cross-validation was used to estimate both the prediction error and the optimal number of factors to be used in the PCR model. This procedure involved the removal of validation samples from the original set of samples, the construction of PCR models (that use different numbers of factors) from the remaining samples, and the use of these models to estimate the HDPE percentage values for the removed samples. The prediction error (RMSEP), for each number of factors, was estimated as the root-mean-square of the differences between the known HDPE percentages and estimated HDPE percentages, for the removed samples only. The optimal number of factors in the PCR model was determined as the number at which the addition of another factor did not greatly decrease the RMSEP. Two separate cross-validation analyses were done, and the reported RMSEP is simply the average of the individual values obtained from the two cross-validation analyses. Figure 1 shows the sample selection for the two cross-validation analyses.

It was found that the first two principal components obtained from the PCR calibration model had to be rotated to enable better interpretation of the model. This rotation was done as described in other references,<sup>16,19</sup> with the use of a LOTUS-123 spreadsheet routine. It should also be noted that one of the five 0% HDPE samples was removed from the analysis, because the error of its PCR-estimated HDPE % value was found to be unusually large.

For the sample rotation study, the NIR spectra were first corrected by the MSC method and then analyzed by principal component analysis<sup>20</sup> (Unscrambler, CAMO A/S, Trondheim, Norway).

## THEORY

**Principal Component Regression.** The principal component regression method, as well as similar multivariate calibration techniques, has been discussed in other references.<sup>21,22</sup> Only the aspects of the method that pertain to this work will be briefly reviewed.

Given the spectral responses at several wavelengths, each obtained from several calibration samples (contained in the matrix *X*), a PCR model is constructed that describes the spectral data in *X* in terms of a linear combination of orthogonal factors:

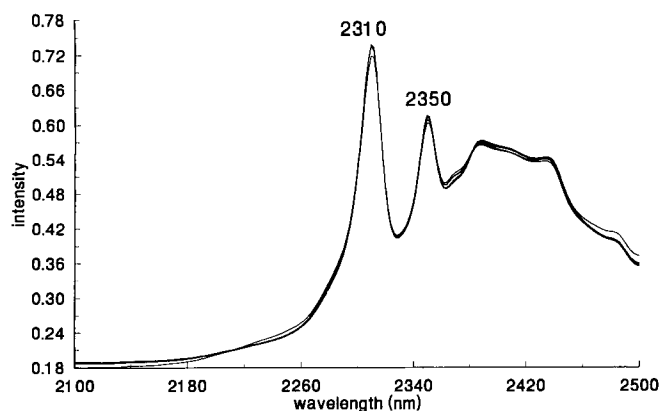


Fig. 2. MSC-corrected NIR spectra of some of the PE blend samples.

$$\mathbf{X} = \mathbf{t}_1\mathbf{p}_1^t + \mathbf{t}_2\mathbf{p}_2^t + \dots + \mathbf{t}_n\mathbf{p}_n^t + \mathbf{E} \quad (1)$$

where the vectors  $\mathbf{t}_1, \mathbf{t}_2, \dots, \mathbf{t}_n$  are the PCR scores for factors 1 to  $n$ , the vectors  $\mathbf{p}_1, \mathbf{p}_2, \dots, \mathbf{p}_n$  are the PCR loadings for factors 1 to  $n$ , and  $\mathbf{E}$  contains the model residuals. The optimal number of factors to be used in the PCR model ( $n$ ) can be determined by several methods, including cross-validation (described in the previous section). If the vector called  $\mathbf{y}$  contains the known values of the property of interest for all the calibration samples, PCR calibration can then be done by multiple regression of the PCR scores ( $\mathbf{t}_1, \mathbf{t}_2, \dots, \mathbf{t}_n$ ) onto  $\mathbf{y}$ .

Each factor in the model can be thought of as an abstract phenomenon that is a source of variation in the NIR spectra of the calibration samples. The scores for a single factor can be thought of as the "intensities" of the corresponding abstract phenomenon for each sample, and the loadings for a single factor can be thought of as the "spectral signature" of the corresponding abstract phenomenon. Therefore, the scores for each factor can be used to determine whether the spectroscopy is sensitive to known trends in the samples, and the loadings can be used to better understand how the NIR spectrum is influenced by different properties that vary in the samples. Furthermore, the spectral residuals (in the matrix  $\mathbf{E}$ ), which contain the spectral information for each sample that is not explained by the PCR model, can provide information about the nature of the random spectral information that is not useful for the determination of the property of interest.

It should be noted that each of the abstract phenomena that are explained by each PCR factor often does not correspond to a single chemical or physical property of the samples. However, if sufficient information about the sample design is available, the PCR factors can be rotated so that each factor corresponds more exclusively to a single known property of the samples. Such rotation has been used previously<sup>19,23</sup> to improve the interpretation of multivariate models.

## RESULTS AND DISCUSSION

**Spectral Data.** The MSC-corrected NIR spectra of several of the PE film samples are shown in Fig. 2. The MSC correction procedure was necessary for these data, because significant baseline offset variation between the spectra (presumably caused by scattering variations

TABLE I. Calibration and cross-validation results.

Calibration error (RMSEE)	2.31% HDPE
Optimal number of factors <sup>a</sup>	3
Prediction error (RMSEP) <sup>a</sup>	2.48% HDPE

<sup>a</sup> Determined by cross-validation.

brought about by variations in film condition and film configuration in the sampling part of the spectrometer) and multiplicative variations in the spectra (primarily caused by variations in the sample thickness) were observed to be present.

The two prominent bands at 2310 and 2350 nm correspond to the combinations between the methylene scissoring mode ( $\delta$ ) and the asymmetric methylene stretching ( $\nu_{as}$ ) and symmetric methylene stretching ( $\nu_s$ ) modes, respectively. The numerous bands that are observed in the region 2360 to 2500 nm are probably overtones and combinations involving the methylene stretching ( $\nu_s$  and  $\nu_{as}$ ), scissoring ( $\delta$ ), and wagging ( $w$ ) modes, or the result of vibrational resonance effects between various overtone and combination modes involving these vibrations.<sup>24,25</sup> It is interesting to note that only very weak visual differences are observed between the spectra of the different film samples, even though the samples range from 0 to 100% HDPE.

**Calibration and Prediction Statistics.** The results of calibration and cross-validation analyses are summarized in Table I. Cross-validation analysis results indicate that three factors were optimal for the PCR model, which implies that there are three independent sources of variation in the NIR spectra of the PE film samples. The prediction error (RMSEP) estimated from the cross-validation analyses is 2.48% HDPE, which corresponds to the entire 0 to 100% HDPE range. It should be noted that this prediction error provides only a rough estimate of the prediction performance of the NIR method. In a later section, sources of error in this work will be addressed, and possible strategies for improvement of the method performance will be proposed.

**PCR Model Interpretation.** Although the calibration and validation statistics indicate that the NIR method can be used to estimate the percentage of HDPE in PE blend films, it is not yet clear how the NIR method determines this property. Furthermore, it is important to know whether there are other variations in the PE film samples or spectral effects that can interfere with the determination of this property. These issues are addressed through interpretation of the PCR calibration model.

**Analysis of PCR Scores.** As mentioned earlier, the first two of the three factors used in the PCR model had to be rotated in order to improve their interpretability. The amount of spectral variation described by each of the three factors (after rotation) is shown in Table II. It should be noted that the rotation procedure caused the

TABLE II. Amount of spectral variation described by each PCR factor (after rotation).

Factor number	Percentage of spectral variation
1	46.67
2	49.25
3	2.56

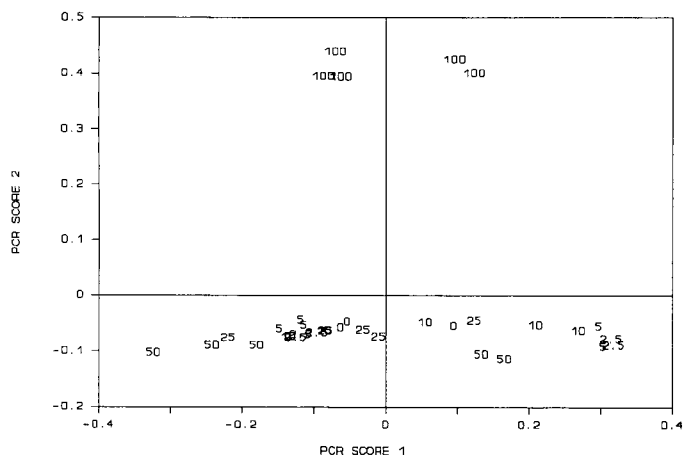


FIG. 3. The PE blend samples represented in the two-dimensional space defined by the first and second PCR scores (after rotation of the original PCR factors). The sample labels refer to the HDPE percentage.

second factor to explain more spectral variation than the first factor, even though this was obviously not the case before the rotation.

The sample scores for the first two PCR factors are shown in Fig. 3. This plot indicates that factor 1 describes a variation between replicate samples of the same composition (for each composition), and factor 2 describes a variation between the 100% HDPE samples and the rest of the samples. It is interesting to note that neither of these factors describes any differences between the samples with different HDPE percentages between 0 and 50% HDPE, even though they together explain almost 96% of the spectral variation. However, observation of the first and third PCR factor scores (Fig. 4) indicates that factor 3 is the most relevant for the determination of HDPE percentage for the samples with 0 to 50% HDPE, even though it explains only 2.56% of the variation in the spectra.

**Variations with HDPE Percentage.** The loading for the second PCR factor, which describes the difference between the 100% HDPE samples and the rest of the samples, is compared to the average calibration spectrum in Fig. 5. This loading spectrum resembles the inverse

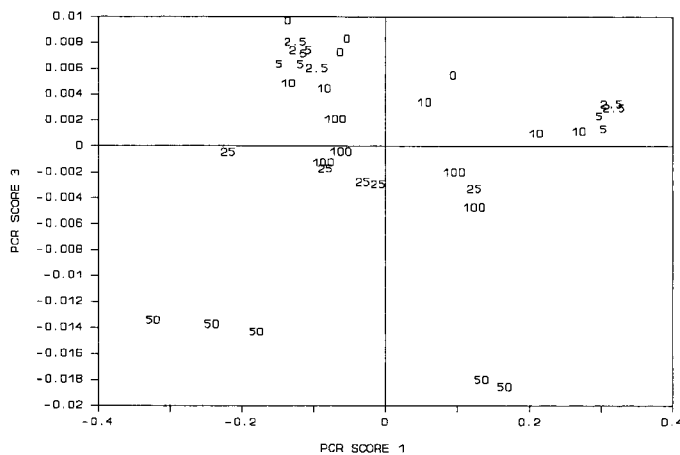


FIG. 4. The PE blend samples represented in the two-dimensional space defined by the first and third PCR scores. The samples refer to the HDPE percentage.

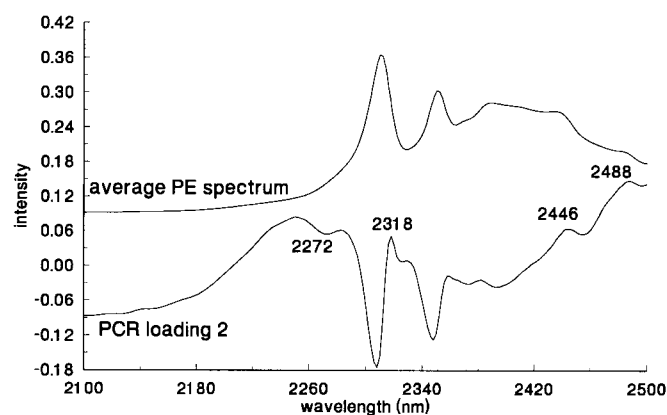


FIG. 5. The loading for the second PCR factor (after rotation), compared to the average of the spectra of the calibration samples.

(or horizontal reflection) of the average spectrum of the PE samples in the region 2260 to 2500 nm, but contains positive peaks of the average spectrum at 2446 and 2488 nm. It has been shown previously<sup>16,19</sup> that such a pattern in a loading spectrum obtained with MSC-corrected NIR spectra (obtained from the InfraAlyzer 500 reflectance spectrometer) could indicate that the factor describes a variation in the scattering ability of the samples. Therefore, because this factor is used to discriminate between the 100% HDPE samples and the other samples, it can be proposed that this discrimination was possible because the 100% HDPE samples have unique scattering properties. Although this proposed mechanism can be confirmed by a simple visual observation of the PE films (the 100% HDPE films appear “whiter” and less transparent than the other films), this analysis provides specific information regarding the sensitivity of MSC-corrected NIR spectra to scattering ability.

More detailed observation of the loading spectrum for factor 2 reveals other spectral effects, in addition to the scattering effect described above. The small negative peak in the loading spectrum at 2272 nm is at the position of a known methyl combination band.<sup>26,27</sup> This observation is expected, because the concentration of methyl groups in the polyethylene blends decreases as the HDPE percentage (or the amount of chain branching) increases. An additional effect in this loading spectrum is the sharp positive band at 2318 nm. The sharpness of this band, and its proximity to the main ( $\nu_{as} + \delta$ ) combination band at 2310 nm, suggests that it corresponds to a special ( $\nu_{as} + \delta$ ) combination band for crystalline PE. Therefore, this band in the loading spectrum probably indicates that the 100% HDPE samples have significantly more crystallinity than the other samples, which is expected from earlier studies.<sup>6</sup> It is interesting to note, however, that it is the scattering effect in the NIR spectrum that appears to be more important than the crystallinity effect or methyl group concentration effect for the discrimination between the 100% HDPE samples and the other samples.

The loading spectrum for PCR factor 3, which explains the difference between the samples with different HDPE % values (for those samples between 0 and 50% HDPE) is shown in Fig. 6. This loading contains positive peaks at 2274 and 2454 nm, which have been previously as-

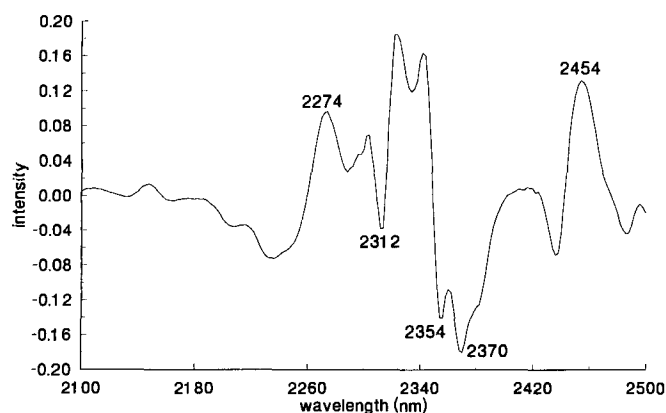


FIG. 6. The loading for the third PCR factor.

signed as methyl group peaks.<sup>26-28</sup> More specifically, these two bands can be attributed to a methyl stretching/bending combination band and second-overtone bending band, respectively. This observation is expected, because (as discussed earlier) the methyl group content should be inversely related to the HDPE percentage.

The sharp negative peak at 2312 nm in the loading spectrum for the third PCR factor (Fig. 6), like the sharp 2318-nm band observed in the loading spectrum for the second PCR factor (Fig. 5), might be a special ( $\nu_{as} + \delta$ ) combination band for crystalline PE. Likewise, another sharp negative peak in the third PCR factor loading at 2354 nm might be a special ( $\nu_s + \delta$ ) combination band for crystalline PE. It is interesting to note that each of these sharp peaks in the loading spectrum is slightly red-shifted from the dominant ( $\nu_{as} + \delta$ ) and ( $\nu_s + \delta$ ) combination bands at 2310 and 2350 nm (Fig. 2). Earlier IR studies of PE<sup>29</sup> indicate that an increase in crystallinity causes an increase in the intensity of two sharp methylene scissoring ( $\delta$ ) bands: one at the high-frequency side and one at the low-frequency side of the broad scissoring band for amorphous PE. Therefore, it is reasonable to suggest that the observed sharp bands at 2312 and 2354 nm in the loading spectrum correspond to a crystalline form of PE in the blends. If this is true, our PCR results indicate that the amount of crystalline PE in the blends increases as the HDPE content increases, which was observed to be true in earlier work.<sup>6</sup>

There are numerous other bands in the third PCR factor loading spectrum which could be attributed to several different properties. For example, the negative peak at 2370 nm is at the same position as a peak that was observed to have significant dichroic activity for NIR studies of oriented PE films.<sup>30,31</sup> In the following section, it will be shown that the light used for the NIR measurements in this work was not randomly polarized, and that this effect in the loading spectrum could therefore indicate a variation in the degree or direction of orientation of the PE polymer chains in the film samples. An additional property that might be represented in this loading is phase segregation of the LDPE and HDPE, which is known to occur for HDPE contents below 50%.<sup>6,32</sup> In fact, it is possible that phase segregation is the primary reason why completely different spectral trends with HDPE percentage are observed for samples between 0 and 50% HDPE and samples between 50 and 100% HDPE. However, further studies of the NIR spectrum

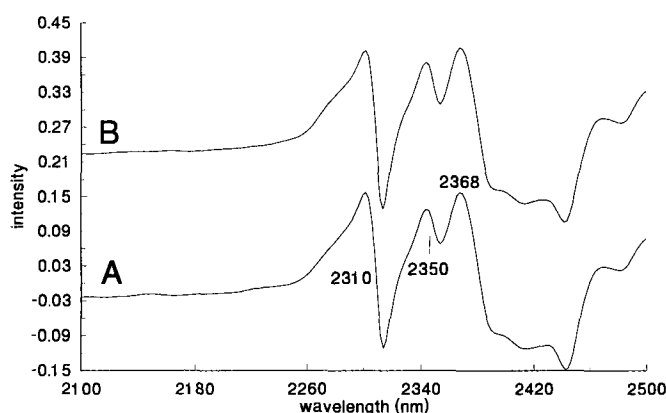


FIG. 7. (A) The loading for the first PCR factor (after rotation); (B) the effect of sample rotation in the sampling compartment of the spectrometer (estimated from principal component analysis of the NIR spectra for all of the samples obtained at four different rotations for each sample).

of PE are necessary to enable a more accurate assessment of the influence of crystallinity, molecular orientation, and phase separation on this analysis.

**Variation between Replicates.** As discussed earlier, PCR factor 1 describes a variation between the replicate samples within each composition. Because this variation accounts for about half the total variation in the NIR spectra of the film samples, it is important to discuss its possible origins. The NIR spectral effect corresponding to this variation, given by the PCR loading for factor 1, is shown in Fig. 7A.

A better understanding of the replicate sample effect can be obtained through observation of the results for the sample rotation study. The PCA results obtained from this study indicate that, for each film analyzed, there exists a unique change in the NIR spectrum from simple rotation of the film sample about the axis of the NIR source beam. Because the film samples were found to have a significant degree of molecular orientation (as determined by viewing the films under polarized visible light), this result indicates that the light used for the NIR measurements was not randomly polarized. Furthermore, if the PCA loading that most closely corresponds to the sample rotation effect (Fig. 7B) is compared to the loading for PCR factor 1 (Fig. 7A), which corresponds to the replicate sample effect in the PCR calibration model, a striking resemblance is obtained. This result indicates that the replicate variation for the calibration samples might be caused by variations in the direction of molecular orientation of the films in the spectrometer, relative to the direction of polarization of the NIR source light. However, it should also be mentioned that an increase or decrease in the *degree* of molecular orientation would also be expected to give a similar spectral effect if the source light was not randomly polarized. Unfortunately, the direction and degree of orientation of the film samples used in this work were not independently determined, and it is therefore difficult to determine the relative contributions of these two similar effects to the replicate variation observed in the PCR calibration model. However, it is important to note that the PCR method was able to model this interfering replicate effect, and thus enable accurate predictions of the HDPE % values of the samples.

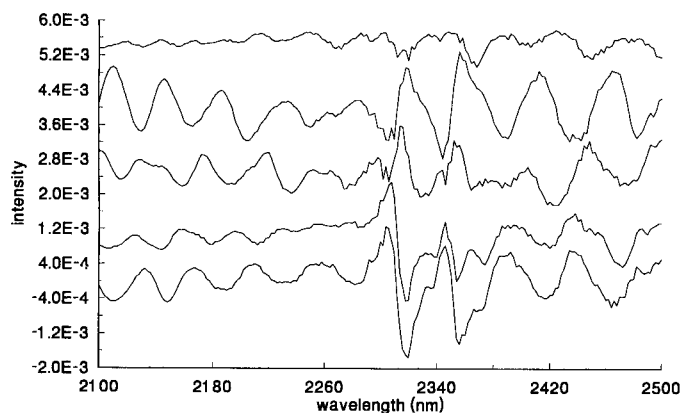


FIG. 8. Spectral residuals of calibration for five of the calibration samples.

In light of the above discussion, the loading for PCR factor 1 could indicate the NIR spectral sensitivity to two phenomena: (1) rotation of the orientation axis of the PE film relative to the polarization direction of the NIR source light, and (2) changes in the conformation of the methylene groups that accompany changes in the degree of molecular orientation. For a given vibrational mode, the sensitivity to the first phenomenon is often referred to as the dichroic sensitivity.

The first-derivative features at 2310 and 2350 nm in the loading spectrum for PCR factor 1 (Fig. 7A) indicate shifts in the two strong bands at these wavelengths (Fig. 2). If it is assumed that these bands correspond to the  $(\nu_{as} + \delta)$  and  $(\nu_s + \delta)$  modes, respectively, the shifts in these bands might be the result of the dichroic sensitivity of the  $\delta$  mode<sup>33</sup> or the sensitivity of the  $\delta$  mode to conformation of the methylene groups in the polymer chains.<sup>34</sup> The strong positive peak at 2368 nm is at the same position as a band that was previously observed to have a large dichroic sensitivity.<sup>30,31</sup> As discussed by Glatt and Ellis,<sup>30</sup> this band probably corresponds to the  $(\nu_s + w)$  mode. If this is the case, then this band would also be expected to be sensitive to methylene group conformation, on the basis of earlier studies of the  $w$  mode.<sup>29,34</sup> However, it should be noted that vibrational resonance effects<sup>24,25</sup> are expected to complicate the spectra in this region, thus making accurate peak assignment difficult.

**Interference Fringes.** Significant sources of random spectral variations in this analysis can be revealed through observation of the spectral residuals (E in Eq. 1), for some of the calibration samples (Fig. 8). These residuals indicate typical interference fringe patterns, which are superimposed on some spectral structure and noise. This result indicates that, although interference fringes were not visually observable in the raw data (Fig. 2), they were present as a weak variation in the spectra. Furthermore, because these fringes appear in the residuals, rather than in the PCR model loadings, they are considered to be a source of random variation in the spectra.

Interference fringes are commonly encountered in the IR spectra of thin films<sup>35,36</sup> and are caused by the interference of light waves that are reflected at different points along the depth of the sample. For this experiment, in which the light transmitted through the film sample is reflected back by the gold-reflecting background, it is expected that no interference fringes would be observed,

because all light that is incident on the sample (except that which is absorbed) should be returned to the detector. However, weak fringes were observed anyway, presumably as a result of small inefficiencies in the gold-reflecting background and light collection optics of the spectrometer.

If the frequency and phase angle of the interference fringes are the same for each sample, then the interference fringe effect over all samples can be explained by a single linear PCR factor and, therefore, incorporated into the PCR calibration model as an interfering effect. However, this does not appear to be the case for this analysis, because the frequencies of the fringe patterns in the spectral residuals were observed to vary from sample to sample. These variations were probably the result of variations in the refractive indices, thicknesses, and surface roughnesses of the PE film samples. Consequently, the fringes of all samples could not be explained by a single PCR factor, and were thus treated as random spectral error. Therefore, from a calibration point of view, the fringes increased the "noise" of the spectral data, thus degrading the prediction performance of the calibration.

**Possible Improvements of the NIR Method.** Although the NIR method described here can be precise enough for many applications, there are several ways in which the method performance could be improved. For example, the use of the weight percentage of HDPE fed into the extruder as the property of calibration might be of practical interest, but could have resulted in errors for the HDPE % values of the actual film samples that were used for the NIR calibration. Such errors would most likely have come from sample nonhomogeneities caused by phase segregation of the HDPE and LDPE before extrusion. Therefore, the use of reference analytical analyses of the identical samples that are used for NIR calibration could result in improved performance of the calibration.

Regarding the interference fringe problem stated earlier, there are several special experimental and instrumental procedures that could be used to suppress such fringes.<sup>36,37</sup> Experimental suppression methods, such as the use of refractive index matching liquids and roughening of the film surface, might not be suitable for non-destructive process and quality analysis. However, instrumental methods, such as the use of plane-polarized light, an IR-cavity accessory, or other special optical arrangements, would be more appropriate for such analyses.

It should also be noted that substantial improvement in the NIR method performance would also be expected if films thicker than 50 to 80  $\mu\text{m}$  are analyzed. Earlier NIR work has shown that quantitative analyses of laminate films up to 250  $\mu\text{m}$  thick can be done with the use of the NIR reflective-transmission method in the region of 2100 to 2500 nm.<sup>16</sup> Not only would the use of thicker films result in enhanced spectral signals, but it would also result in the reduction of interference fringes, which, in this case, would cause a significant decrease in the amount of useless random variation in the spectra.

Finally, because the NIR response to HDPE percentage is nonlinear (in that different spectral trends are used to determine this property for HDPE contents above and below 50%), a nonlinear calibration modeling approach

might produce better results. Such nonlinear approaches, including artificial neural networks<sup>38,39</sup> and locally weighted regression,<sup>40,41</sup> have been shown to perform more accurate predictions than linear multivariate methods in cases where nonlinearities are present.

## CONCLUSION

This study has shown that NIR spectroscopy in the region 2100 to 2500 nm, combined with multivariate calibration techniques, can be used to determine the composition of thin film blends of high-density and low-density polyethylene. For the samples containing 50 to 100% HDPE, NIR spectral effects of scattering, and perhaps the degree of crystallinity, are used to determine the HDPE percentage. However, for the samples containing 0 to 50% HDPE, spectral effects of the methyl group concentration, and probably the degree of crystallinity, are used to determine the HDPE percentage.

It was found that a variation between replicate samples was responsible for almost half the variation in the NIR spectra of the film samples. Through observation of the PCR model loadings and the results of a model experiment, this variation was attributed to variations in both the direction and degree of molecular orientation in the samples. Unfortunately, the relative contributions of these two effects to the replicate variation could not be determined. In addition, it should be noted that the sensitivity of the NIR method to the direction of molecular orientation in the film samples was brought about by the fact that the NIR source light was not randomly polarized.

Weak, but significant, interference fringes were found to be present in the NIR spectra of the films. Because these fringes vary in their frequency, and therefore cannot be explained by a single linear PCR factor, they contribute to the random error in the spectral data, which ultimately limits the prediction ability of the calibration model.

The prediction performance of the NIR method described in this work is not necessarily indicative of the performance of the method for more specific applications. Substantial improvements in the method as described in this work could be made through optical or experimental suppression of the interference fringes, more accurate reference analyses, and the use of nonlinear calibration modeling. In addition, it is expected that NIR spectroscopy in the same spectral region would perform better if samples thicker than those used in this study (50 to 80  $\mu\text{m}$ ) were used, because the spectral signal would be enhanced and interference fringe-based noise would be greatly reduced.

## ACKNOWLEDGMENTS

The samples used for this work were provided by STAT-OIL (Stathelle, Norway), and important information regarding the samples was provided by Dr. Arne Hendriksen. The author acknowledges a postdoctoral fellowship from the Royal Norwegian Council for Scientific and Industrial Research.

1. J. Stepek, V. Duchacek, D. Curda, J. Horacek, and M. Sipek, *Polymers as Materials for Packaging* (Ellis Horwood Ltd., Chichester, 1987).

2. F. A. Paine and H. Y. Paine, *A Handbook of Food Packaging* (Leonard Hill, Glasgow, 1983).
3. M. Mathlouthi, *Food Packaging and Preservation* (Elsevier, London, 1986).
4. J. Martinez-Salazar, M. Sanchez-Cuesta, and J. Plans, *Polymer* **32**, 2984 (1991).
5. J. Martinez-Salazar, M. Sanchez-Cuesta, and F. J. Balta Calljea, *Colloid Polym. Sci.* **265**, 239 (1987).
6. D. C. Yang, J. M. Brady, and E. L. Thomas, *J. Mater. Sci.* **23**, 2546 (1988).
7. H. W. Siesler and K. Holland-Moritz, *Infrared and Raman Spectroscopy of Polymers* (Marcel Dekker, New York, 1980).
8. H. W. Siesler and K. Holland-Moritz, *Infrared and Raman Spectroscopy of Polymers* (Marcel Dekker, New York, 1980), pp. 118–129.
9. G. F. Kirkbright and K. R. Menon, *Anal. Chim. Acta* **136**, 373 (1982).
10. M. Ganzarolli de Oliveira, O. Pessoa, H. Vargas, and F. Galembeck, *J. Appl. Poly. Sci.* **35**, 1791 (1988).
11. C. E. Miller, *Appl. Spectrosc. Rev.* **26**, 275 (1991).
12. E. Stark, K. Luchter, M. Margoshes, *Appl. Spectrosc. Rev.* **22**, 335 (1986).
13. D. D. Archibald, C. E. Miller, L. T. Lin, and D. E. Honigs, *Appl. Spectrosc.* **42**, 1549 (1988).
14. B. Feldhaeuser, K. Meya, and H. W. Siesler, in *Proc. SPIE-INT Soc. Opt. Eng.* **1145** (Int. Conf. Fourier Transform Spectroscopy, 7th), 158 (1989).
15. A. M. C. Davies, A. Grant, G. M. Gavrel, and R. V. Steeper, *Analyst* **110**, 643 (1985).
16. C. E. Miller, S. A. Svendsen, and T. Næs, *Appl. Spectrosc.*, paper to appear in **47**(3) (1993).
17. C. E. Miller, "NIR—More than a Non-invasive Composition Sensor: Applications to Polymeric Food Packaging," in *Proc. 5th Intl. Conf. on NIR Spectrosc.*, Haugesund, Norway, (1992), in press.
18. P. Geladi, D. MacDougall, and H. Martens, *Appl. Spectrosc.* **39**, 491 (1985).
19. C. E. Miller and B. E. Eichinger, *J. Appl. Poly. Sci.* **42**, 2169 (1991).
20. I. J. Joliffe, *Principal Component Analysis* (Springer-Verlag, New York, 1986).
21. H. Martens and T. Næs, *Multivariate Calibration* (Wiley, Chichester, 1989), pp. 97–116.
22. H. Martens and T. Næs, "Multivariate Calibration by Data Compression," in *Near-infrared Technology in the Agricultural and Food Industries*, P. Williams and K. Norris, Eds. (American Association of Cereal Chemists, St. Paul, Minnesota, 1987).
23. W. Windig and H. L. C. Meuzelaar, in *Computer Enhanced Analytical Spectroscopy*, H. L. C. Meuzelaar and T. L. Isenhour, Eds. (Plenum, New York, 1987), pp. 81, 82.
24. J. L. Duncan, *Spectrochim. Acta* **47A**, 1 (1991).
25. P. R. Griffiths, in *Proc. 5th Intl. Conf. on NIR Spectrosc.*, Haugesund, Norway, (1992), in press.
26. C. E. Miller, *Appl. Spectrosc.* **43**, 1435 (1989).
27. H. V. Druschel and F. A. Iddings, *Anal. Chem.* **35**, 28 (1963).
28. T. Takeuchi, S. Tsuge, and Y. Sugimura, *Anal. Chem.* **41**, 184 (1969).
29. H. Hagemann, R. G. Snyder, A. J. Peacock, and L. Mandelkern, *Macromolecules* **22**, 3600 (1989).
30. L. Glatt and J. W. Ellis, *J. Chem. Phys.* **19**, 449 (1951).
31. L. Glatt and J. W. Ellis, *J. Chem. Phys.* **15**, 884 (1947).
32. P. Barham, M. J. Hill, A. Keller, and C. C. A. Rosney, *J. Mater. Sci. Lett.* **7**, 1271 (1988).
33. Y. Uemura and R. S. Stern, *J. Poly. Sci.*, A-2, **10**, 1691 (1972).
34. R. G. Snyder, *J. Chem. Phys.* **47**, 1316 (1967).
35. R. Kronig, *Textbook of Physics* (Pergamon, London, 1954), pp. 379–382.
36. R. F. Edgar and B. J. Stay, *SPIE Infrared Technology and Applications* **590**, 316 (1985).
37. P. H. Hindle, *Paper Technology and Industry* **25**, 77 (1984).
38. R. L. Long, V. G. Gregoriou, and P. J. Gemperline, *Anal. Chem.* **62**, 1791 (1990).
39. T. Næs, K. Kvaal, T. Isaksson, and C. Miller, *J. Chemometrics*, submitted 1992.
40. T. Næs, T. Isaksson, and B. Kowalski, *Anal. Chem.* **62**, 664 (1990).
41. T. Næs and T. Isaksson, *Appl. Spectrosc.* **46**, 34 (1992).